

## General Disclaimer

### One or more of the Following Statements may affect this Document

- This document has been reproduced from the best copy furnished by the organizational source. It is being released in the interest of making available as much information as possible.
- This document may contain data, which exceeds the sheet parameters. It was furnished in this condition by the organizational source and is the best copy available.
- This document may contain tone-on-tone or color graphs, charts and/or pictures, which have been reproduced in black and white.
- This document is paginated as submitted by the original source.
- Portions of this document are not fully legible due to the historical nature of some of the material. However, it is the best reproduction available from the original submission.

# DMSK: A Practical 2400-bps Receiver for the Mobile Satellite Service

An MSAT-X Report

Faramaz Davarian  
Marvin Simon  
Joe Sumida

(NASA-CR-176194) DMSK: A PRACTICAL  
2400-BPS RECEIVER FOR THE MOBILE SATELLITE  
SERVICE: AN MSAT-X REPORT (Jet Propulsion  
Lab.) 42 p HC A03/MF A01 C5CL 17B

N85-35324

g3/32 Unclas  
27478

June 15, 1985

**NASA**

National Aeronautics and  
Space Administration

Jet Propulsion Laboratory  
California Institute of Technology  
Pasadena, California



# **DMSK: A Practical 2400-bps Receiver for the Mobile Satellite Service**

**An MSAT-X Report**

**Faramaz Davarian  
Marvin Simon  
Joe Sumida**

June 15, 1985



National Aeronautics and  
Space Administration

**Jet Propulsion Laboratory**  
California Institute of Technology  
Pasadena, California

The research described in this publication was carried out by the Jet Propulsion Laboratory, California Institute of Technology, under a contract with the National Aeronautics and Space Administration.

Reference herein to any specific commercial product, process, or service by trade name, trademark, manufacturer, or otherwise, does not constitute or imply its endorsement by the United States Government or the Jet Propulsion Laboratory, California Institute of Technology.

## ABSTRACT

This report investigates the practical aspects of a 2400-bps differential detection minimum-shift-keying (DMSK) receiver. Fundamental issues relating to hardware precision, Doppler shift, fading, and frequency offset are examined, and it is concluded that the receiver's implementation at baseband is more advantageous both in cost and simplicity than its IF implementation.

The DMSK receiver has been fabricated and tested under simulated mobile satellite environment conditions. The measured receiver performance in the presence of anomalies pertinent to the link is presented in this report. Furthermore, the receiver behavior in a band-limited channel (GMSK) is also investigated.

The DMSK receiver performs substantially better than a coherent minimum-shift-keying (MSK) receiver in a heavily fading environment. The DMSK radio is simple and robust, and results in a lower error floor than its coherent counterpart. Moreover, this receiver is suitable for burst-type signals, and its recovery from deep fades is fast.

This work was performed for the mobile satellite experiment under a NASA contract.

## ACKNOWLEDGMENT

The authors would like to acknowledge the efforts of J. Packard in the implementation and testing of the DMSK receiver.

## CONTENTS

I.	INTRODUCTION . . . . .	1
II.	THE TWO-BIT DIFFERENTIAL RECEIVER . . . . .	3
III.	RECEIVER PERFORMANCE IN THE ABSENCE OF FREQUENCY UNCERTAINTY . . . . .	9
	A. The Receiver Error Performance . . . . .	11
	B. The Error Floor . . . . .	14
IV.	RECEIVER PERFORMANCE IN THE PRESENCE OF FREQUENCY OFFSET . . . . .	14
	A. Optimum Receiver Bandwidth in the Presence of Frequency Offset . . . . .	20
	B. Frequency Tracking . . . . .	22
V.	SIGNAL BAND-LIMITING . . . . .	28
VI.	RESULTS . . . . .	31
	REFERENCES . . . . .	35

### Figures

1.	The DMSK Receiver Block Diagram for Two-Bit Differential Detection . . . . .	4
2.	The DMSK Receiver Baseband Implementation . . . . .	8
3.	The Measured Eye Diagram of the 2400-bps Signal . . . . .	10
4.	The DMSK Measured Static Error Performance . . . . .	12
5.	The DMSK Measured Error Performance in the Presence of Fading . . . . .	13
6.	The Error Floor as a Function of LMR in a Mobile Satellite Link with $f_d = 72$ Hz . . . . .	15
7.	The Phase Distortion $\epsilon$ as a Function of the Filter Bandwidth-Time Product $BT$ . . . . .	17
8.	The Measured Eye Diagram in the Presence of Doppler Shift with:	
	(a) $f_d = 20$ Hz . . . . .	19
	(b) $f_d = 72$ Hz . . . . .	19

Figures (Contd.)

9.	The Two-Bit DMSK Receiver with the AFC, AGC, and Bit-Synchronization Loops in Operation . . . . .	23
10.	The Receiver Error Performance in the Presence of a Frequency Error of 100 Hz (curve A), with AFC (curve B), and with AFC in the absence of a frequency error (curve C) . . . . .	26
11.	The Receiver Performance Under the Worst-Case Rician Model with LMR = 10 and $f_d = 72$ Hz . . . . .	27
12.	The Error Rate, as a Function of $E_b/N_0$ , for GMSK (BT = 0.5) in the Presence of a 100-Hz Doppler Shift . . . . .	29
13.	The GMSK (BT = 0.5) Signal Performance in the Presence of Rayleigh and Rician Fading . . . . .	30

Tables

1.	Normalized $m$ in dB as a Function of $\delta$ . . . . .	21
2.	Optimum BT and Improvement on $m$ as a Function of $\delta$ . . . . .	22
3.	Phase-Locked Loop Design . . . . .	32
4.	Static and Dynamic Power Performance of the Receiver . . . . .	33



## I. INTRODUCTION

The Mobile Satellite Service (MSS) is a new concept in mobile communications whereby the service subscribers can initiate or receive calls almost anywhere in the U.S. and Canada using low-cost, low-power mobile terminals. The broad coverage of this service will become possible via utilization of one or more geostationary satellites. Therefore, the spacecraft can be perceived as being a transmission tower that has a clear view of the continent because of its enormous height.

Employing spaceborne platforms for mobile communications objectives is not without its drawbacks. Indeed, a spectrum shortage, which is due to the limited frequency-reuse capability of MSS, and a power shortage are the major challenges facing the network designer. Many techniques must be carefully examined and improved before consideration for MSS; in particular, digital modulation requires special attention. The candidate transceiver must conform to the characteristics of the mobile environment as well as to the features of the satellite. In short, spectral and power efficiency must be combined with agility and robustness. Furthermore, physical compactness and low cost must also be achieved.

Studies conducted by the National Aeronautics and Space Administration (NASA) [1] have suggested that low bit-rate transmission is suitable for the MSS applications, particularly from the frequency and power conservation point of view. Moreover, the particular bit rate of 2400 bits per second (bps) is emphasized due to its applicability to the Linear Predictive Coding (LPC) of speech and its usefulness for message transmission of a typical size such as

1000 bits. Since, due to practical reasons beyond the scope of this report to discuss, the network structure will be of the Single Channel Per Carrier (SCPC), Frequency Division Multiple Access (FDMA) type, a small channel spacing is desirable for the sake of spectrum optimization. Therefore, the need for a high-performance, narrowband digital transceiver is apparent. This report will describe one such implementation, which utilizes the spectrum efficiency of the Minimum-Shift-Keying (MSK) approach for modulation on one hand, and the responsiveness and robustness of differential detection techniques for demodulation on the other.

MSK and its enhanced version, Gaussian MSK (GMSK), have recently been the subject of many studies for mobile communications applications [2]. In addition, their viability for moderate-rate data transmission over mobile channels has been demonstrated [3]. In principle, there are three distinct methods of signal detection that can be applied to MSK/GMSK signals: coherent, differentially coherent (known as DMSK), and noncoherent. The noncoherent detector, in essence, is an FM limiter/discriminator receiver. This receiver tries to use the FM nature of MSK for signal demodulation. However, due to the small size of the frequency deviation, the discriminator type of receivers for MSK has not gained popularity [4]. At the other extreme, the coherent demodulation approach results in the best performance if the channel is ideal. In practice, the multipath effect plagues the carrier-phase tracking loop dramatically, resulting in a suboptimal performance. Nevertheless, for moderate-rate links, e.g., 32 kbps, the coherent detector has been shown to be feasible [5]. At our bit rate of interest, 2400 bps, the coherent technique suffers from a large dynamic loss coupled with an excessively high error floor [4].

The differential detection technique, i.e., DMSK, has gained increased popularity in recent years, particularly because of its simplicity. This technique has been successfully applied to data communication over multipath fading channels for transmission rates as low as 16 kbps, but lower bits rates, such as 2400 bps, posed an implementation difficulty that had to be overcome. This report describes a new baseband approach to this technique.

## II. THE TWO-BIT DIFFERENTIAL RECEIVER

A version of this DMSK receiver was first suggested by Masamura et al. in 1979 [6]. The receiver block diagram is illustrated in Fig. 1. Note that the name "two-bit differential detector" arises from the use of a  $2T$ -delay line in the circuit, where  $T$  denotes the bit time. Although the receiver can also be implemented with a one-bit delay, this report deals only with the two-bit version. After the initial suggestion, this receiver became the subject of many investigations [7], including an in-depth analysis by Simon and Wang [8, 9].

The two-bit differential receiver determines the excess phase of an MSK signal over a two-bit period. In the ideal case, this phase is either zero or  $\pm\pi$ . Hence, it can be seen that extreme phase response linearity or group delay flatness is demanded from both the IF filter and the delay line (see Fig. 1) to ensure phase integrity.

The MSK signal that creates an excess phase of  $\pm\pi/2$  every bit time can be formulated as

$$s(t) = A \cos [\omega_0 t + \phi(t)] \quad (1)$$

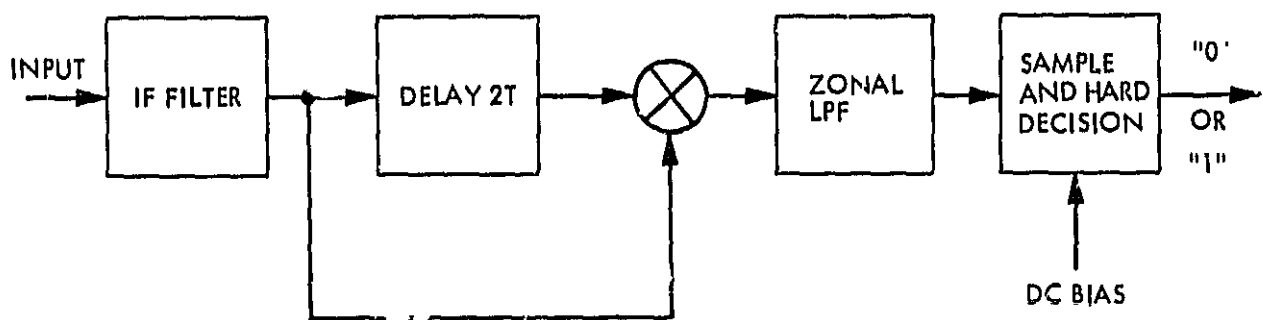


Fig. 1. The DMSK Receiver Block Diagram for Two-Bit Differential Detection

where  $\omega_0$  denotes the carrier angular frequency and  $\phi(t)$  denotes the excess phase. Ignoring the noise and the intersymbol interference (ISI) generated by the LP filter, the demodulated signal can be expressed as

$$r(t) = s(t)s(t - 2T) = A^2 \cos[2\omega_0 T + \phi(t) - \phi(t - 2T)] \quad (2)$$

Now let  $\Delta\phi = \phi(t) - \phi(t - 2T)$  and assume<sup>1</sup>

$$2\omega_0 T = 2K\pi \quad (3)$$

where  $K$  is an integer. Hence, Equation (2) can be written as

$$r(t) = A^2 \cos(\Delta\phi) \quad (4)$$

The MSK excess phase at the  $i^{\text{th}}$  sampling instance is given by

$$\Delta\phi_i = \begin{cases} +\pi & a_i = a_{i-1} \\ 0 & a_i \neq a_{i-1} \end{cases} \quad (5)$$

where  $a_i$  denotes the  $i^{\text{th}}$  bit. Now viewing the MSK as a frequency-shift-keying (FSK) signal, a change in data, i.e.,  $a_i \neq a_{i-1}$ , means a change in the transmitted frequency by  $\pm 1/(2T)$ . Hence, a ripple or error in the group delay response of the receiver can have catastrophic results. Let  $d$  denote

---

<sup>1</sup> This is a key assumption at low bit rates and has ramifications in terms of such system parameters as allowable Doppler shift and local oscillator offset.

the peak-to-peak differential delay for the two tones at frequencies  $f_0 + 1/(4T)$  and  $f_0 - 1/(4T)$ , where  $f_0$  is the receiver IF frequency. Hence, when  $a_i \neq a_{i-1}$ , an additional phase error may propagate through the system, degrading  $\Delta\phi$  to

$$\Delta\phi_i = \begin{cases} \pm\pi & a_i = a_{i-1} \\ \cos(\Psi) & a_i \neq a_{i-1} \end{cases}$$

where

$$\Psi = 2\pi f_0 d \quad (6)$$

To reduce the distortion caused by the imperfect system phase response, the product  $f_0 d$  must be minimized.

It has been shown that to optimize the receiver power performance, the receiver's IF bandwidth must be approximately equal to the data bit rate [8]. In fact, this bandwidth provides the best balance between noise and ISI. Hence, for the bit rate of interest, the receiver's IF bandwidth is approximately 2400 Hz. The narrowband requirement of the receiver's filter prohibits a very flat group-delay response. Indeed, for this IF filter, it is rather impractical to reduce the peak-to-peak delay distortion below 20  $\mu\text{s}$ .<sup>2</sup> Using this value in Equation (6), an upper bound on the phase distortion can be

---

<sup>2</sup> Specifications were provided by Alpha Components, Inc., Mechanicsburg, Pennsylvania, July 1984.

determined for a given IF frequency. To do so, we assume a very low IF frequency of 10 kHz; hence,

$$\psi = 2\pi \times (2 \times 10^{-5}) \times 10^4 = 72 \text{ deg}$$

A phase error of this magnitude will severely distort the receiver's eye opening, resulting in a drastic loss of performance, particularly if the effect of ISI is also considered.

To eradicate this problem and still maintain the restriction shown in Equation (3), the baseband implementation of Fig. 2 is used. In this figure, the IF bandpass filter is replaced by two baseband filters that band-limit the noise in the in-phase and quadrature signal paths. The actual low-pass filters used had a Gaussian characteristic and their peak-to-peak delay differential was 17  $\mu\text{s}$  within the passband.<sup>3</sup> The maximum peak-to-peak differential delay of the delay lines is only 5  $\mu\text{s}$ . Hence,

$$\psi = 2\pi(17 + 5) \times 10^{-6} \times 600 = 4.7 \text{ deg}$$

where 600 Hz is the baseband frequency of the FSK tone. Hence, only a small maximum phase error is associated with this receiver implementation. The above phase error can cause only a negligible eye-opening distortion. Moreover, in practice, the error will very seldom become as large as 4.7 deg.

---

<sup>3</sup> This is easily achieved at baseband, whereas the 20- $\mu\text{s}$  differential delay at IF is very difficult to achieve.

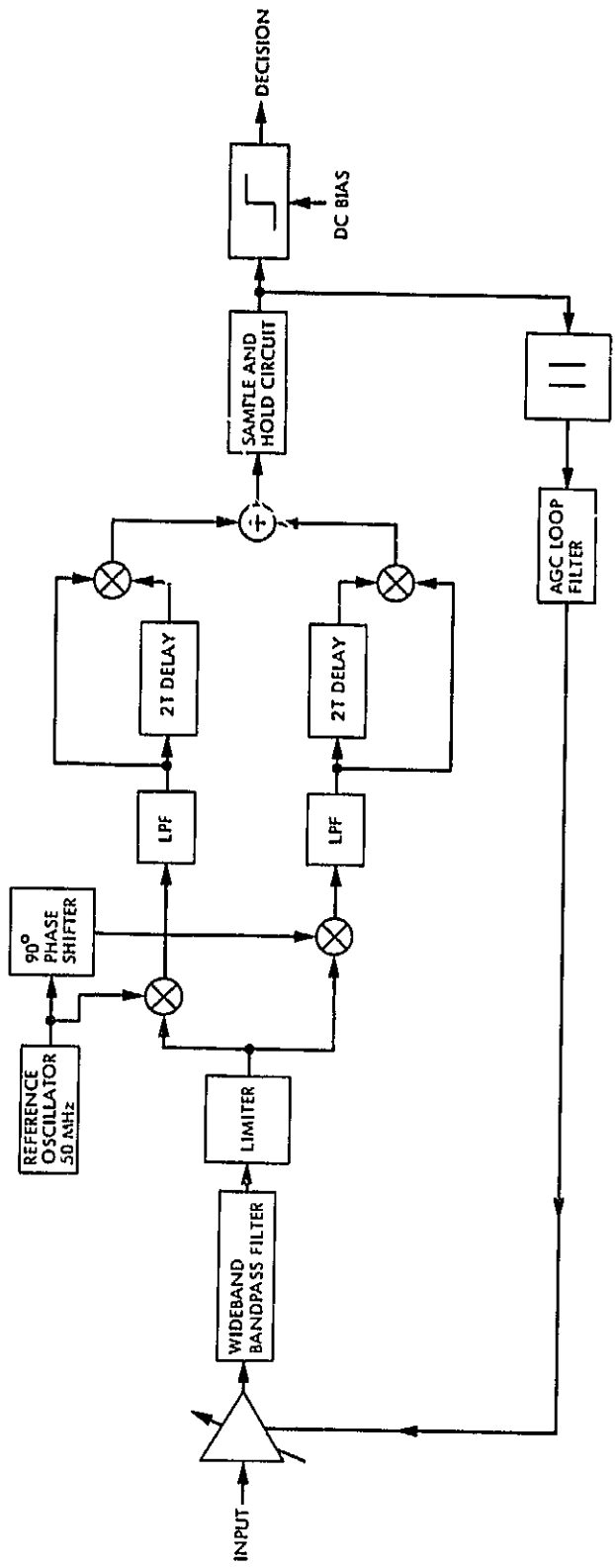


Fig. 2. The DMSK Receiver Baseband Implementation



To demonstrate the receiver's design viability and examine the hardware component's precision, i.e., the noise-limiting filters and the delay lines, the eye diagram of the demodulated signal as captured by an oscilloscope is shown in Fig. 3. The large eye opening is a testimony to a skillful hardware design and implementation.

### III. RECEIVER PERFORMANCE IN THE ABSENCE OF FREQUENCY UNCERTAINTY

It is known that differentially coherent receivers demonstrate sensitivity to large frequency offsets. The receiver performance in the presence of frequency uncertainty will be treated in Section IV. Section III focuses on determining the system performance in the presence of noise and multipath fading. The results presented in this section were obtained experimentally using the Mobile Satellite (MSAT) hardware channel simulator. The architecture and functions of this link simulator have been described previously [10].

The receiver's static and dynamic responses have been determined analytically in [9]; however, no clue to its error floor is provided. The irreducible error rate or error floor is an artifact observed in mobile channels. In some cases, this anomaly can severely undermine the link performance. The tests performed on this receiver had the following goals:

- (1) Determine the receiver performance in noise.
- (2) Determine the fade margin for both terrestrial (Rayleigh model) and satellite (Rician model) mobile channels.
- (3) Determine the error floor in the presence of multipath fading.

ORIGINAL PAGE IS  
OF POOR QUALITY

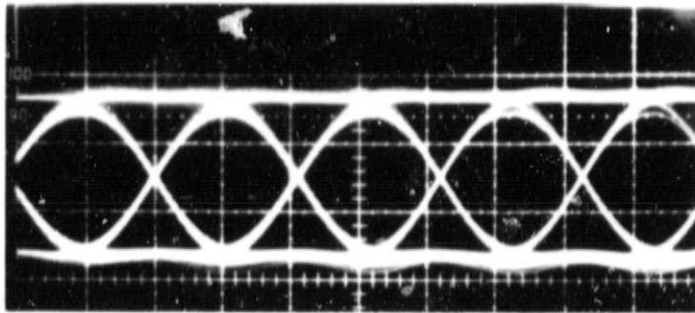


Fig. 3. The Measured Eye Diagram of the 2400-bps Signal

- (4) Test the receiver robustness and responsiveness to a burst-like signal.
- (5) Evaluate the receiver in the presence of frequency uncertainty (this topic will be discussed in Section IV).

#### A. The Receiver Error Performance

The results of these tests are primarily presented in the form of error rate curves as functions of average  $E_b/N_0$ . Starting with the static performance, Fig. 4 shows the receiver's measured error performance in the presence of thermal noise. The solid curve in this figure shows the ideal performance extracted from [8]. The two curves are very close, indicating insignificant implementation loss.

Figure 5 illustrates the receiver performance in the presence of Rayleigh and Rician fading with  $f_d$  (Doppler frequency) equal to 20 and 72 Hz,<sup>1</sup> respectively. For the Rician case, it was assumed that the line-of-sight-to-multipath ratio (LMR) is 10. This particular value of LMR represents a typical Rician condition in the rural area, which was obtained from the propagation experiments conducted in the U.S. [11]. These experiments were aimed at characterizing the MSAT link. Note that the effect of the satellite in the link is two-fold, namely, the reduction of both the fade margin and the error floor. For example, the fade margin at a bit error probability of  $P_e = 0.001$  is 3 dB for the satellite-aided link, whereas the same error probability lies below the performance limit of a terrestrial link (see Fig. 5).

<sup>1</sup>These are typical Doppler shifts that a vehicle communicating in the 800 MHz band will experience.

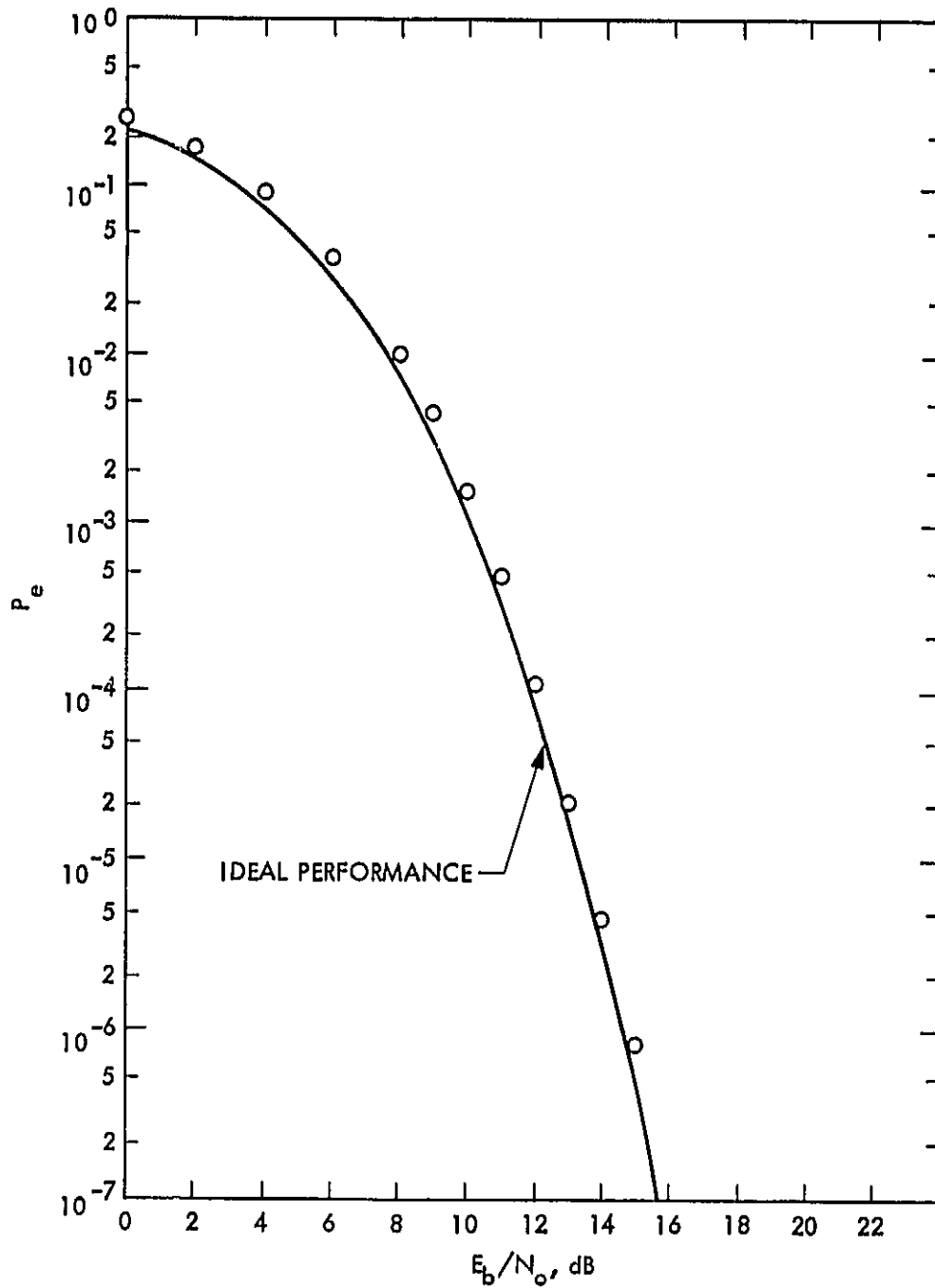


Fig. 4. The DMSK Measured Static Error Performance

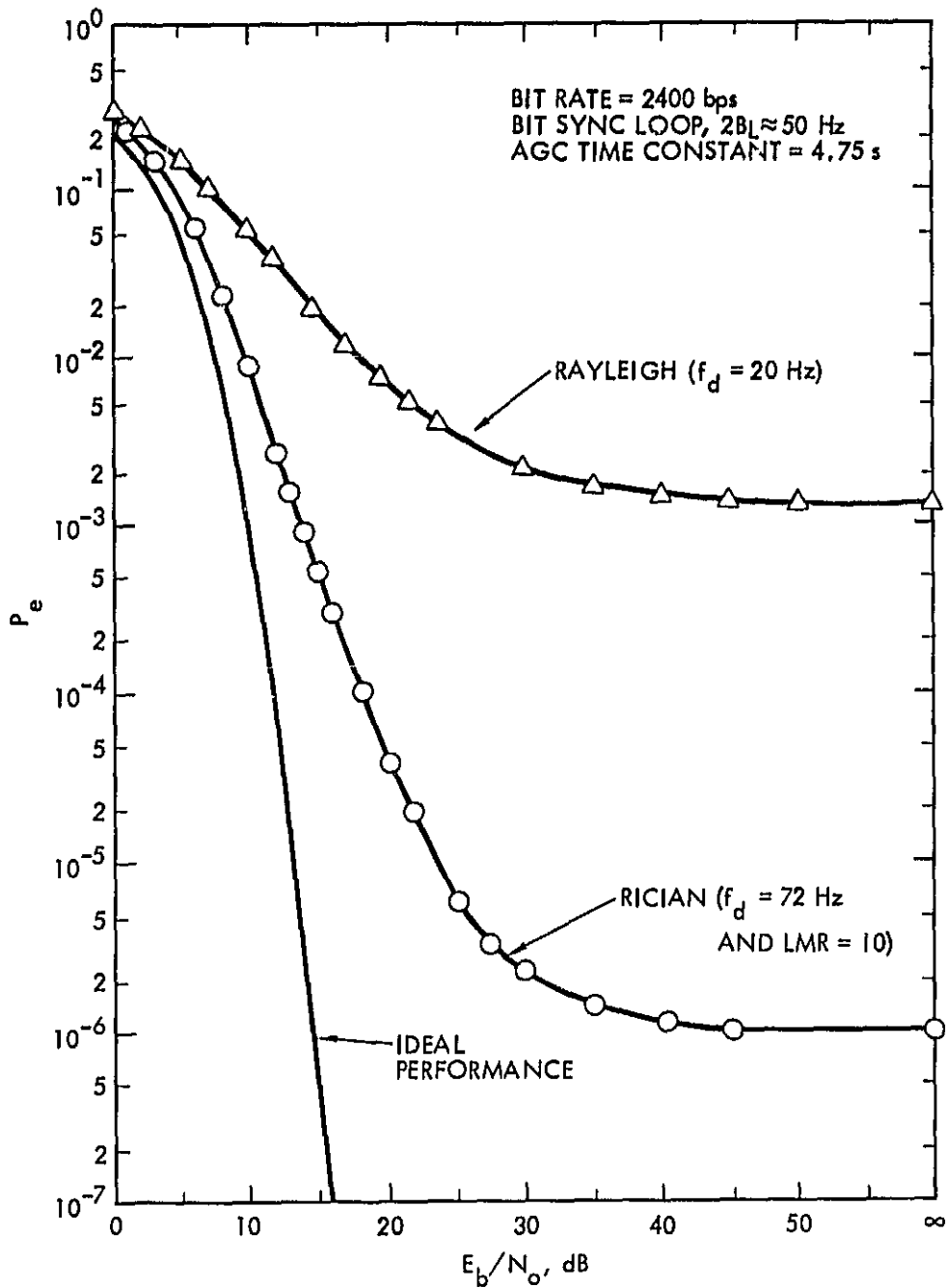


Fig. 5. The DMSK Measured Error Performance in the Presence of Fading

## B. The Error Floor

The error floor associated with the 2400-bps signaling rate in a high-frequency band such as 800 MHz poses a formidable obstacle for mobile communications via terrestrial channels. Often, frequency efficiency must be greatly sacrificed to restrict this floor below a desired threshold. For the satellite-aided links, however, the existence of a strong line-of-sight (LOS) component can be helpful in controlling the link's irreducible error rate. To verify this concept, the error floor of the DMSK receiver was measured for a range of channel characteristics with  $f_d = 72$  Hz, and is shown by curve A of Fig. 6. This figure shows the irreducible error rate as a function of LMR. It should be recognized that a large LMR, i.e., larger than 13 dB, constitutes a reasonably stable (nonfading) link, whereas a small LMR, i.e., less than -3 dB, constitutes a heavily fading (Rayleigh) link [12]. At LMR = 10 dB, the irreducible error rate is  $10^{-6}$ . This error floor is well below the network requirement ( $P_e = 10^{-3}$ ) for digital voice communications.<sup>4</sup>

## IV. RECEIVER PERFORMANCE IN THE PRESENCE OF FREQUENCY OFFSET

To understand the influence of a frequency offset on the two-bit differential receiver, the effect of the noise-limiting filters on the eye opening of the received waveform must be examined. The signal at the baseband end of the receiver is described by Equation (4), where  $\Delta\phi$  denotes the excess phase

---

<sup>4</sup> This information was provided by Time and Space Processing, Inc., Santa Clara, California.

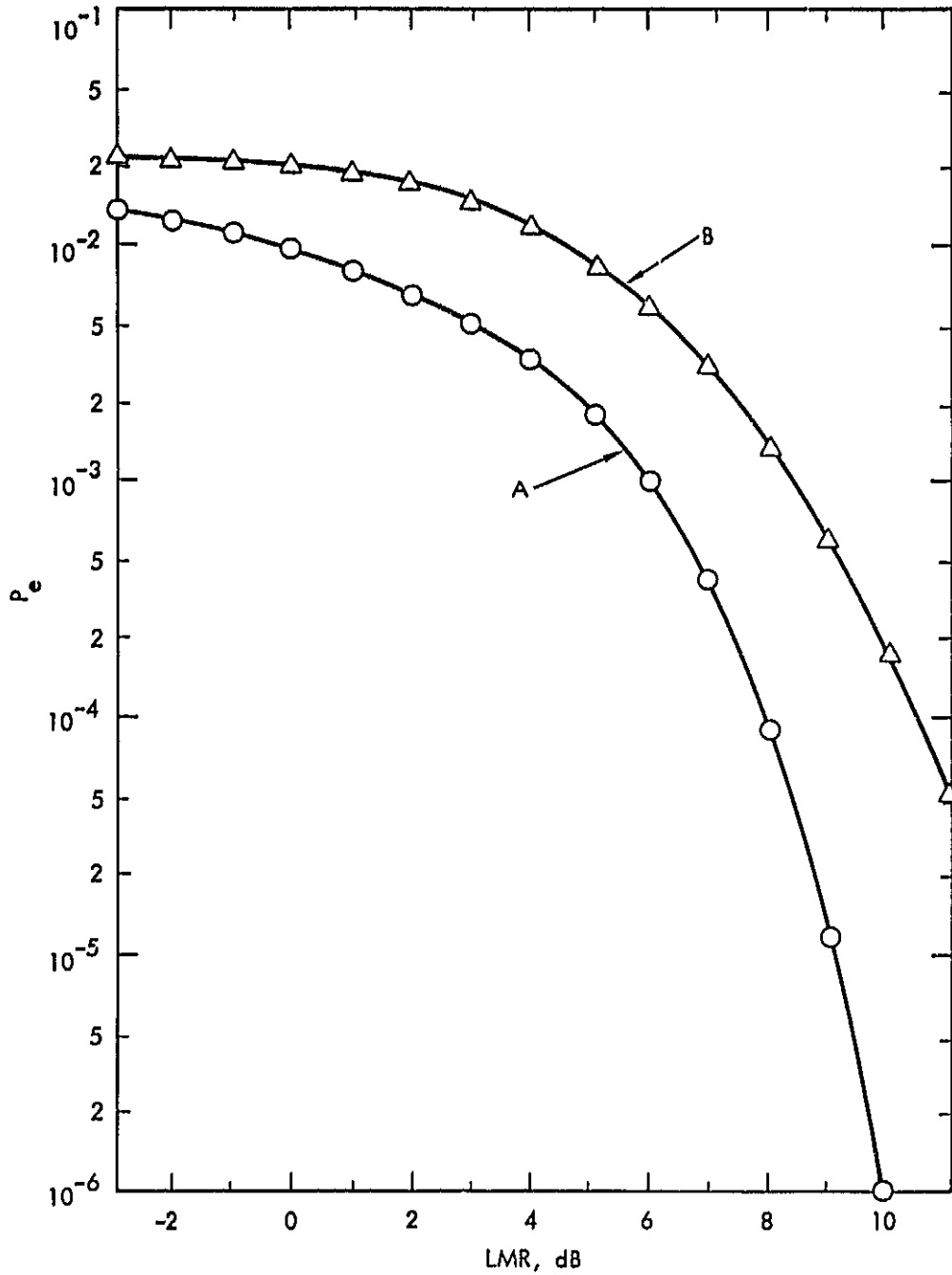


Fig. 6. The Error Floor as a Function of LMR in a Mobile Satellite Link with  $f_d = 72$  Hz. Curve A was obtained using the conventional model, and curve B was obtained using the worst-case model.

gain over a  $2T$  period and its value at the sampling time is given by Equation (5) when the ISI created by the receiver filters is ignored. Consideration of the ISI effect modifies the values given in Equation (5) to the following:

"0" was transmitted:

$\Delta\phi$	Probability
0	0.5
$\epsilon$	0.25
$-\epsilon$	0.25

"1" was transmitted

$\Delta\phi$	Probability
$-\pi$	0.125
$-\pi + 2\epsilon$	0.125
$-\pi + \epsilon$	0.25
$\pi$	0.125
$\pi - 2\epsilon$	0.125
$\pi - \epsilon$	0.25

Assuming the filters are of Gaussian characteristics with bandwidth  $B$ ,  $\epsilon$  is given by [8]

$$\epsilon = (\pi/4) - \arctan \frac{(13/15) \exp [-\pi/(8 \times BT \times BT)]}{1 - (2/15) \exp [-\pi/(2 \times BT \times BT)]} \quad (7)$$

Note that for  $BT = \infty$ ,  $\epsilon = 0$ . A plot of  $\epsilon$  versus  $BT$  is illustrated in Fig. 7. Of particular interest is the value of  $\epsilon$  at  $BT = 0.9$ , since it is shown in [8] that this value of  $BT$  results in the optimum performance for the receiver. For this value of  $BT$ ,  $\epsilon = 16.5$  deg.



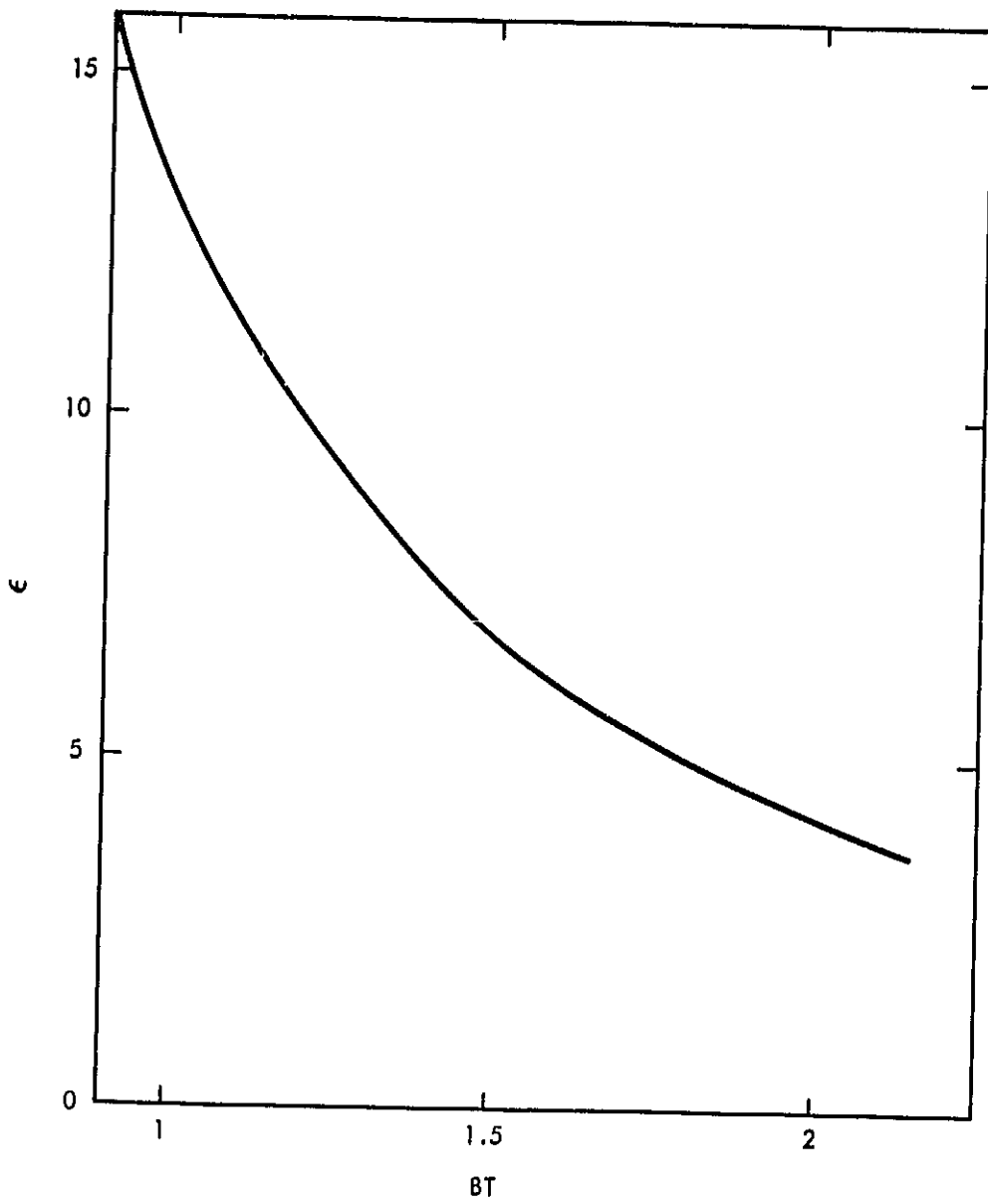


Fig. 7. The Phase Distortion  $\epsilon$  as a Function of the Filter Bandwidth-Time Product  $BT$

The presence of Doppler and/or local oscillator offset further reduces the data eye opening. The phase error  $\delta$  produced because of a frequency difference of  $\Delta f$  is given by

$$\delta = 2T (2\pi \times \Delta f) \quad (8)$$

Therefore, the sampled signal is proportional to the following quantities:

"0" was transmitted:

<u>Quantity</u>	<u>Probability</u>
$\cos( \delta )$	0.5
$\cos( \delta  +  \epsilon )$	0.25
$\cos( \delta  -  \epsilon )$	0.25

"1" was transmitted:

<u>Quantity</u>	<u>Probability</u>
$-\cos( \delta )$	0.25
$-\cos( \delta  +  \epsilon )$	0.25
$-\cos( \delta  -  \epsilon )$	0.25
$-\cos( \delta  + 2 \epsilon )$	0.125
$-\cos( \delta  - 2 \epsilon )$	0.125

Observing the above tabulated values, it is clear that the eye opening is asymmetric. The two values  $-\cos(|\delta| + 2|\epsilon|)$  and  $-\cos(|\delta| - 2|\epsilon|)$  are present for a "1" transmission, whereas their images do not exist for a "0" transmission. Therefore, a "1" results in a smaller noise margin than a "0." This asymmetry issue is discussed in great detail in [9].

To visually observe the eye diagram distortion, the receiver eye patterns for two Doppler values of 20 and 72 Hz were recorded using an oscilloscope and are shown in Figs. 8(a) and 8(b), respectively. The asymmetric nature of the

ORIGINAL PAGE IS  
OF POOR QUALITY

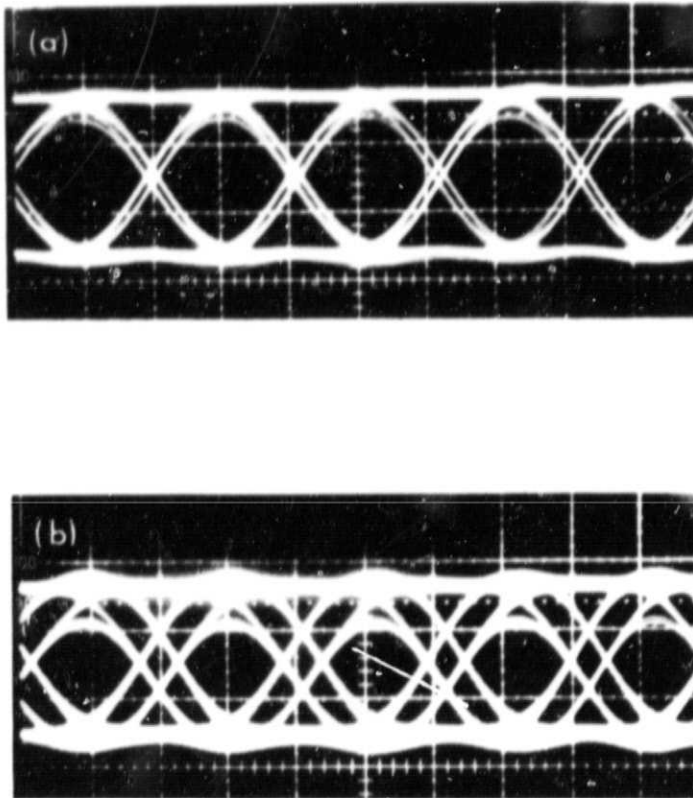


Fig. 8. The Measured Eye Diagram in the Presence of Doppler Shift with:  
(a)  $f_d = 20$  Hz, and (b)  $f_d = 72$  Hz

eye pattern is evident from these figures. The eye opening is substantially reduced at 72 Hz, whereas this loss is negligible at 20 Hz. It is important to note that the sign of the frequency offset does not affect the direction in which the closure of the eye occurs. Hence, it is expected that offsetting the detection threshold can lessen the distortion caused by the frequency uncertainty.

The effect of a frequency uncertainty on the receiver performance can also be reduced by increasing the receiver's bandwidth. This approach is investigated in the following subsection.

#### A. Optimum Receiver Bandwidth in the Presence of Frequency Offset

As mentioned earlier, it is shown in [8] that the optimum balance between thermal noise and the closing of the eye occurs at  $BT = 0.9$ . In the presence of frequency uncertainty, however, this value of  $BT$  does not present the best balance between noise and signal distortion. Since at moderate and high signal-to-noise ratios the receiver performance is primarily determined by the smallest eye opening, the following ratio may be selected as the figure of merit ( $m$ ) for the two-bit DMSK receiver:

$$m = \frac{\cos^2 (|\delta| + 2|\epsilon|)}{BT} \quad (9)$$

The numerator of the above ratio is an indication of the worst-case eye opening, and the denominator is proportional to the noise power. Hence, it is desirable to maximize  $m$ . Table 1 shows  $m$  as a function of  $\delta$ , where  $m$  is normalized to its value at  $\delta = 0$ . For example, a loss of about 4 dB is expected when

Table 1. Normalized m in dB as a Function of  $\delta$

$\delta$ (deg)	m
0	0
5	-0.54
10	-1.2
15	-2
20	-2.9
25	-4
30	-5.3
35	-7

$\delta = 25$  deg. To reduce this loss, a new BT that maximizes m in the presence of frequency uncertainty can be used. Table 2 shows the gains for m relative to its value at BT = 0.9. Note that modification of BT adversely affects the frequency error-free performance only by a small quantity. For instance, if BT is increased to 1.2, a loss of 0.3 dB occurs relative to BT = 0.9 when no frequency error exists.

From the above discussion it is concluded that in the presence of frequency offset, moderate improvements can be expected by (1) slight offsetting of the detector threshold, and (2) increasing the receiver bandwidth. The next section presents a third method of combatting frequency uncertainty, a method that is more powerful than the previous two, particularly for large frequency errors.

Table 2. Optimum BT and Improvement on m as a Function of  $\delta$

$\delta$ (deg)	New BT <sup>a</sup>	Improvement (dB)
0	0.9	0
5	1	0.08
10	1.1	0.2
15	1.1	0.4
20	1.2	0.7
25	1.3	1.2
30	1.4	1.8
35	1.5	2.6
40	1.6	3.8
45	1.7	5.7
50	1.9	9

<sup>a</sup> Optimized for the given  $\delta$ .

## B. Frequency Tracking

Combination of the Doppler shift and the local oscillator uncertainty gives rise to frequency errors with a magnitude too large to be remedied by the simple techniques described above for the bit rate of interest. Therefore, a tracking loop that can correct large frequency errors is required for stable and efficient operation of the receiver. Fortunately, the structure of the receiver at baseband lends itself to incorporation of an automatic frequency control (AFC) loop without substantial added complexity. The block diagram of the receiver with the AFC loop is shown in Fig. 9. Observation of this figure reveals that the loop error signal is proportional to the product of the following two signals (ignoring the ISI generated by the filters):

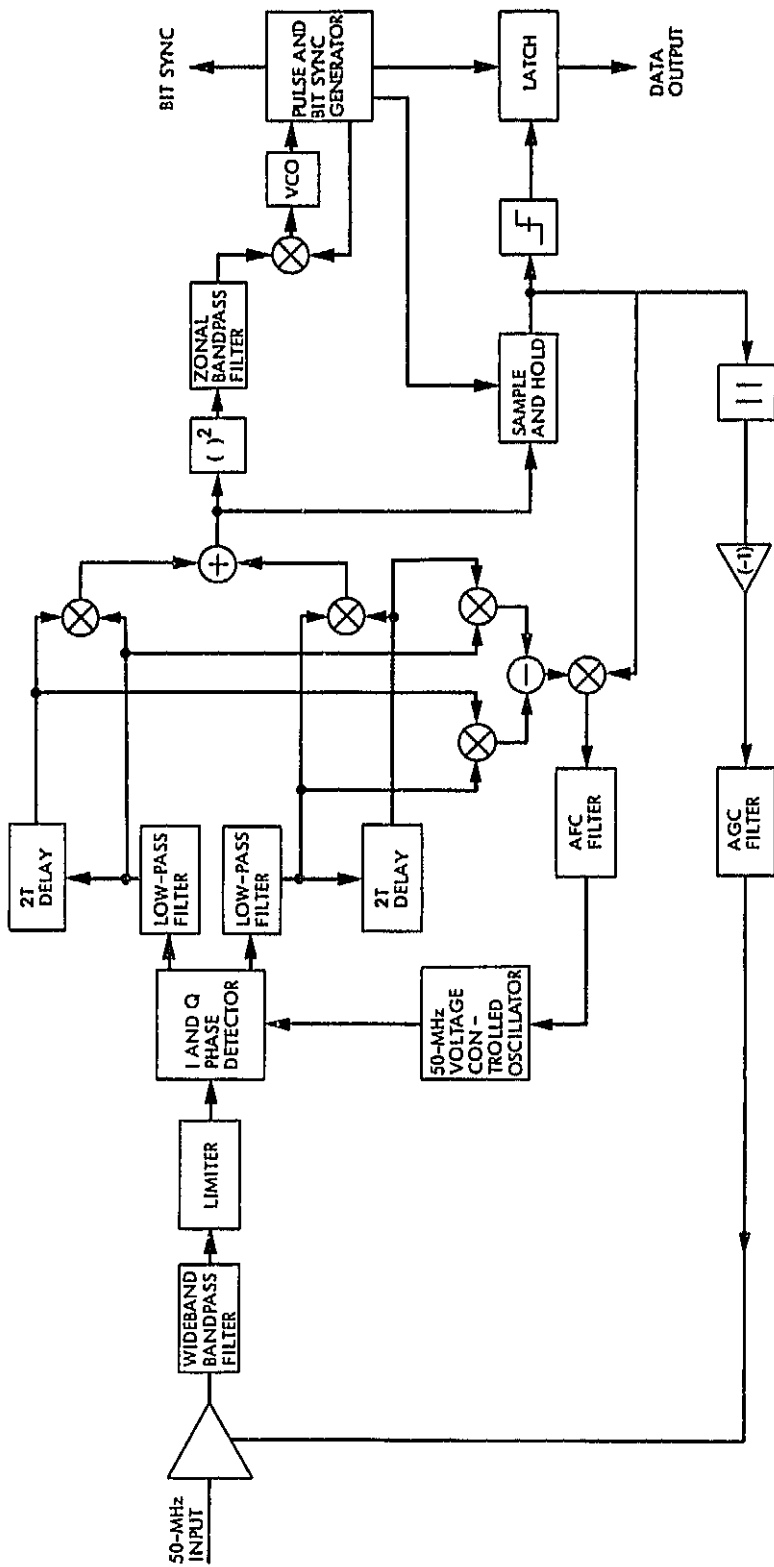


Fig. 9. The Two-Bit DMSK Receiver with the AFC, AGC, and Bit-Synchronization Loops in Operation

$$r_1(t) = \cos(\delta + k\pi)$$

$$r_2(t) = \sin(\delta + k\pi)$$

where  $k = 0$  for a "0" data bit and  $\pm\pi$  for a "1" data bit, and  $\delta$  is given by Equation (8).

Hence, the loop error signal is given by

$$e(t) = 2K \sin(\delta + k\pi) \cos(\delta + k\pi)$$

or

$$e(t) = K \sin(2\delta) \tag{10}$$

where  $K$  is a constant. The error signal,  $e(t)$ , is first smoothed by the loop filter and then used to drive the voltage-controlled oscillator (VCO) to the correct frequency. Note that the error signal is slightly modified in practice due to the ISI generated by the transmit and receive filters.

The theoretical pull-in range of the AFC can be calculated from Equations (8) and (10). To avoid false lock, the argument of the sine function in Equation (10) must be less than  $\pi$ ; hence,

$$2\delta = 2 \times (2T) \times (2\pi) \times \Delta f < \pi$$

or



$$\Delta f < \frac{R_b}{8}$$

Since  $R_b = 2400$ , it is required that  $\Delta f < 300$  Hz. In practice, the pull-in range is less than this value because of the ISI effect.

To demonstrate the effect of the AFC on the receiver, a number of experiments in the presence of a frequency error were conducted. Figure 10 shows the error performance curve as a function of  $E_b/N_0$  in the presence of a 100-Hz frequency offset with and without the AFC loop. At  $P_e = 10^{-4}$ , a 5-dB improvement results from the use of the loop. This figure also demonstrates the static performance (no frequency error) when the loop is used. The performance loss in this case is negligible for low  $P_e$ ; however, for  $P_e = 0.1$ , the loss is about 1 dB.

To explore the effect of the vehicle's motion on the received signal's LOS component, tests were conducted under a Rician model in which the LOS component was shifted in the spectrum by the maximum Doppler shift. In fact, this is a realistic worst-case assumption, since the vehicle is likely to move in a random direction relative to the (satellite) transmitter. The offsetting of the LOS creates additional stress on the receiver. Under this model both the dynamic error rate and the error floor are likely to increase. For example, the error floor of the receiver as a function of LMR when LOS undergoes a Doppler shift of 72 Hz is shown by curve B of Fig. 6 (no AFC).

Figure 11 shows the error probability versus  $E_b/N_0$  for a Rician fading channel with LMR = 10, a Doppler shift of 72 Hz, and LOS also shifted in

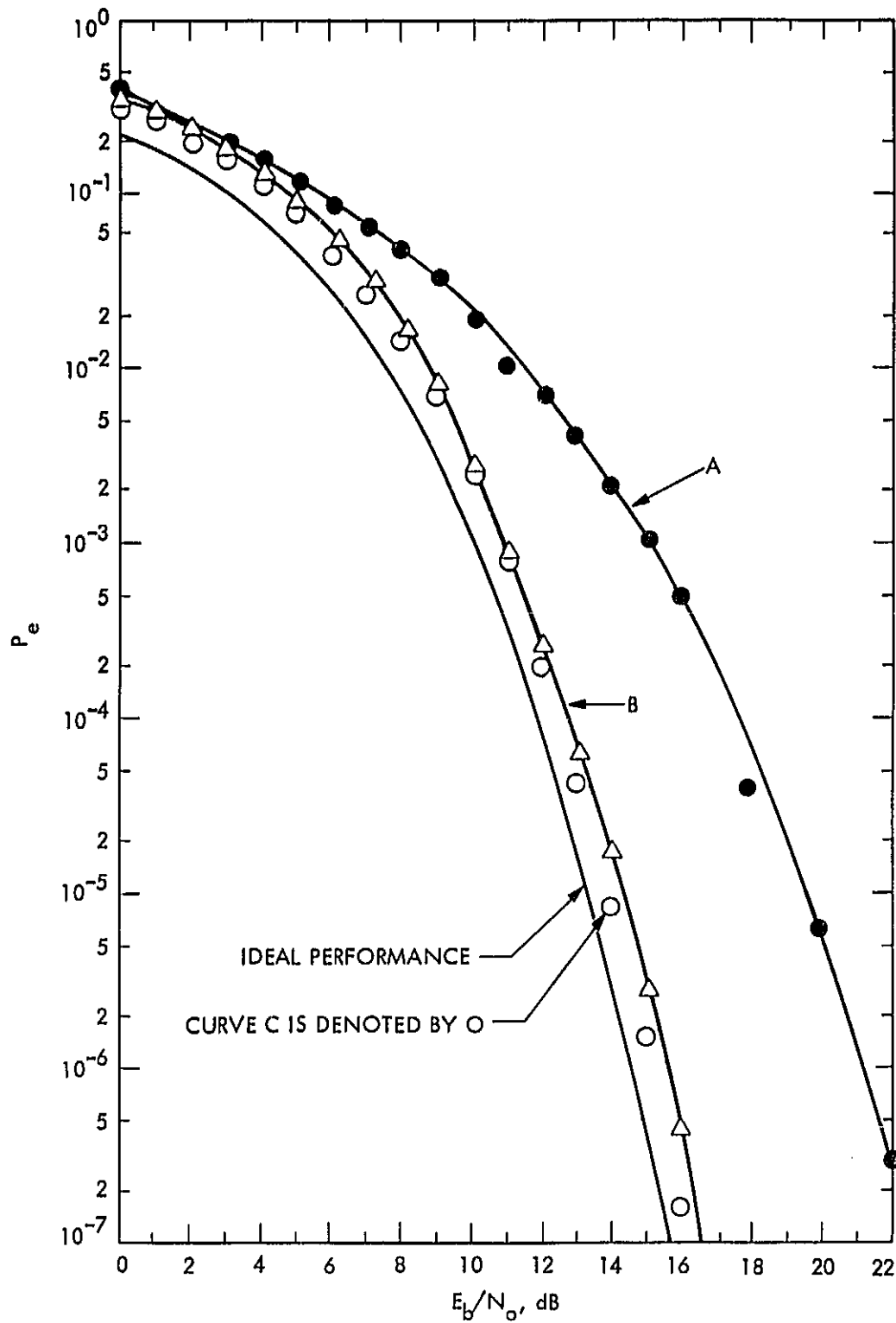


Fig. 10. The Receiver Error Performance in the Presence of a Frequency Error of 100 Hz (curve A), with AFC (curve B), and with AFC in the absence of a frequency error (curve C)

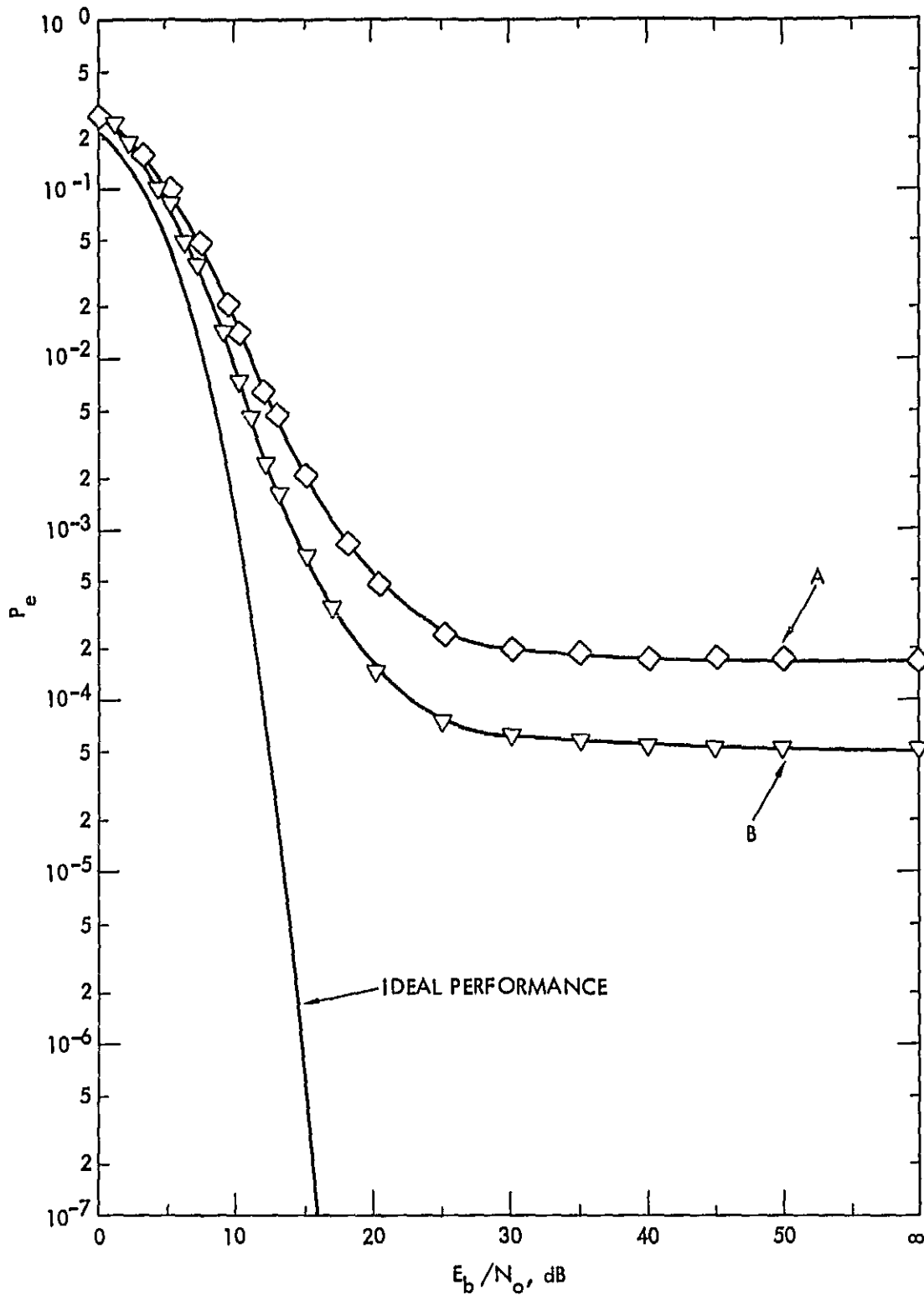


Fig. 11. The Receiver Performance Under the Worst-Case Rician Model with LMR = 10 and  $f_d = 72$  Hz. Curve A was produced without the AFC loop, and curve B with the AFC loop.

frequency by 72 Hz, without the AFC loop (curve A) and with the AFC loop (curve B). The introduction of the AFC loop has improved the dynamic performance by 2.5 dB and the error floor by a factor of 2.

## V. SIGNAL BAND-LIMITING

To conserve bandwidth, often it is desirable to band-limit the signal at the transmitter. If a Gaussian filter is added to the baseband portion of an MSK transmitter, the resulting signal is known as GMSK. The tests described in the previous sections were conducted using a quadrature type of MSK transmitter. To evaluate the receiver's ability to demodulate GMSK signals, an FM type of transmitter was constructed. To introduce signal band-limiting, a baseband Gaussian filter with  $BT = 0.5$  was included that could be switched into the data path. Hence, without the filter the resulting signal was MSK, and with the filter the signal was GMSK. Experience showed that this method of signal generation (FM) creates anomalies that in turn cause a loss of about 1 dB at the receiver. This conclusion was arrived at by using this transmitter in the MSK mode and comparing the results with the ones obtained from using the quadrature type of transmitter. Since the purpose of this report is to evaluate the receiver, no further discussion of the transmitter will be made.

Figure 12 shows the receiver error performance as a function of  $E_b/N_0$  for the GMSK signal and in the presence of a frequency offset of 100 Hz (curve A). Curve B shows the same scenario when the AFC loop is used to track the frequency error. Clearly, a GMSK signal is much more sensitive to frequency errors than an MSK signal. Figure 13 shows the receiver performance in the

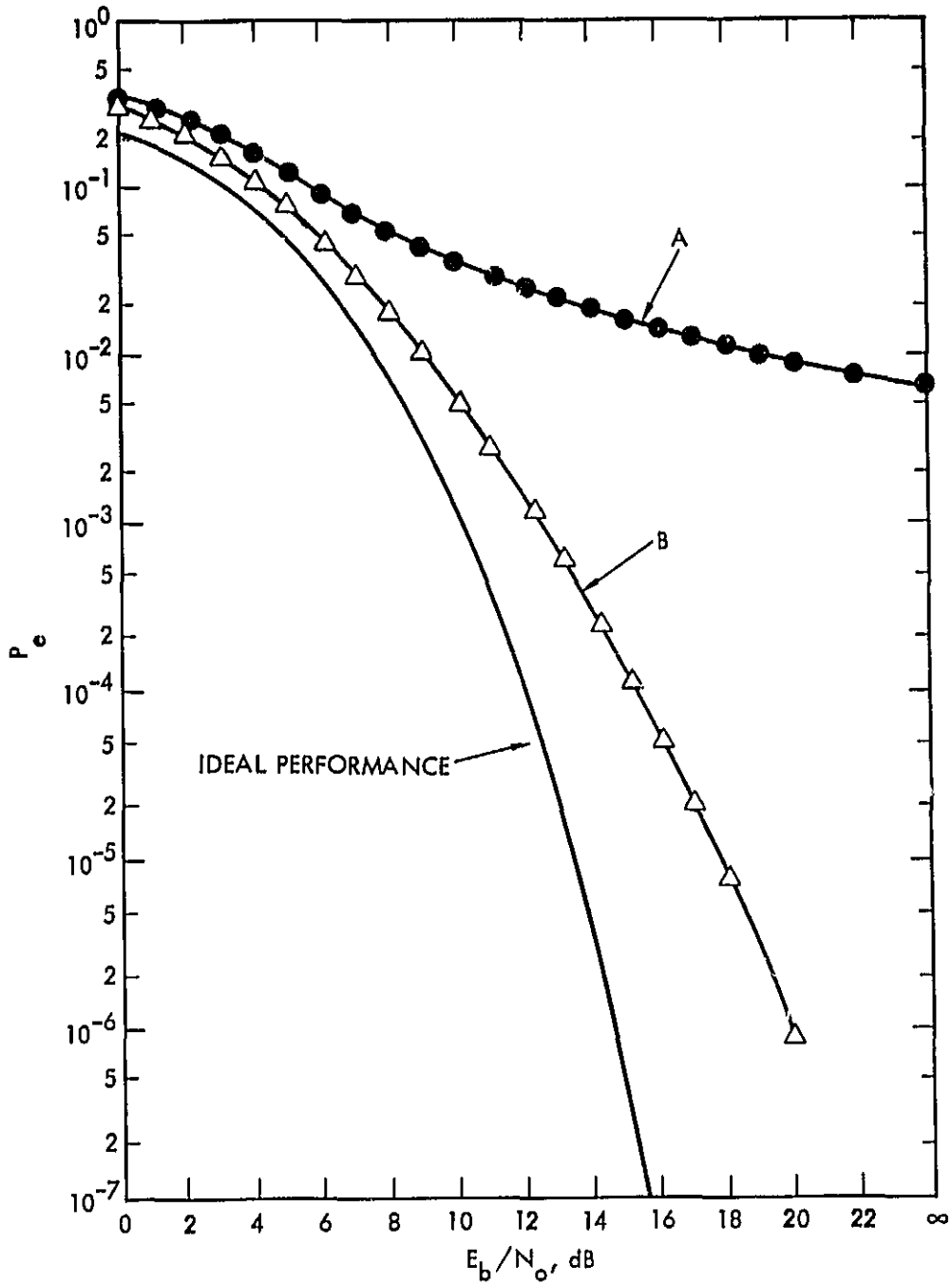


Fig. 12. The Error Rate, as a Function of  $E_b/N_0$ , for GMSK ( $BT = 0.5$ ) in the Presence of a 100-Hz Doppler Shift. Curve A was produced without the AFC loop, and curve B with the AFC loop.

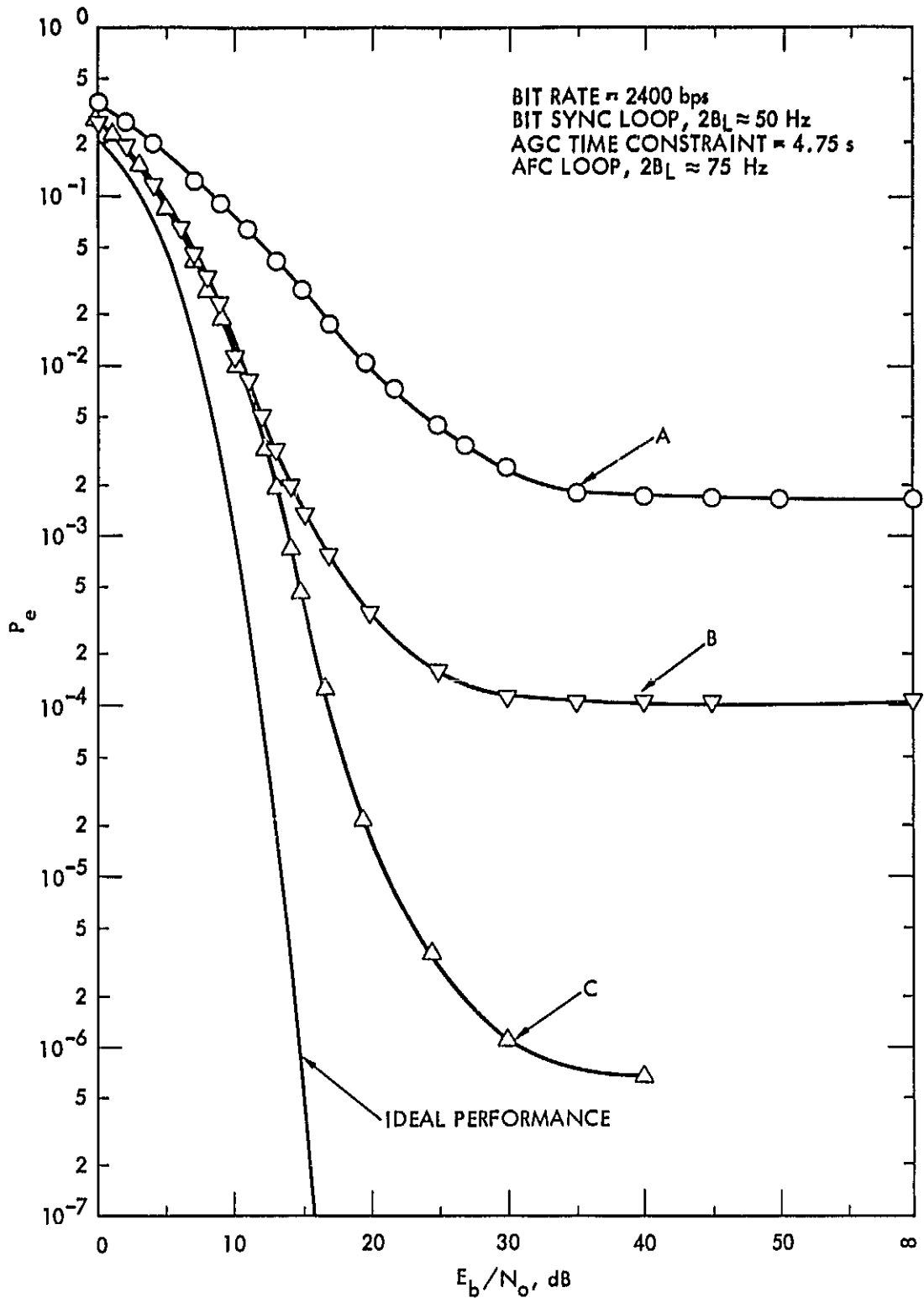


Fig. 13. The GMSK ( $BT = 0.5$ ) Signal Performance in the Presence of Rayleigh and Rician Fading. Curve A shows Rayleigh fading with  $f_d = 20$  Hz; curve B shows Rician fading, using the worst-case Rician model, with  $f_d = 72$  Hz and LMR = 10; and curve C shows Rician fading, using the worst-case Rician model, with  $f_d = 20$  Hz and LMR = 10.

presence of Rayleigh and Rician fading with the AFC. In this figure it is assumed that the LOS is shifted as much as the prevailing Doppler shift, which is a worst-case assumption.

## VI. RESULTS

The baseband implementation of the two-bit differential detector is a viable approach to achieving the 2400-bps data reception in the MSAT environment. This configuration is a receiver for both MSK and GMSK signals. It is robust and is quick to recover from deep fades. This receiver can easily be implemented using VLSI technology, resulting in a low-cost and compact radio that is highly suitable for mobile satellite links. In the absence of large frequency offsets, i.e., offsets larger than 20 Hz, the receiver's recovery time is about one or two milliseconds.

It is shown that the receiver performance degrades severely with a large frequency error, i.e., an error larger than 20 Hz. To combat this anomaly, an AFC loop was designed and added to the receiver. This loop is capable of reducing the frequency error to negligible levels. The cost of the frequency control loop on the static performance of the receiver is about 0.5 dB. Table 3 shows the important loop parameters. Note that, in the presence of this loop, the receiver's acquisition time is increased to about 90 ms for a frequency offset of 250 Hz.

The static and dynamic  $C/N_0$  requirement of the receiver for  $P_e = 0.001$  is summarized in Table 4. This table indicates that in the worst-case situation, in which the signal experiences a Rician fading of 72 Hz and the LOS is

Table 3. Phase-Locked Loop Design

Parameters	Definitions
$F_h = \pm 1,000.00$ Hz	Hold-in range
$F_p = +252.30$ Hz	Pull-in range
$G_o = 6.28E+03$ 1/s	DC loop gain
$F_o = +100.00$ Hz	Frequency offset
$S_e = 0.100$ rad (5.73 deg)	Static phase error
$2B_L = 150.00$ Hz	Two-sided loop noise bandwidth
$K_v = 1.00E+02$ Hz/V	VCO gain
$K_d = 0.159$ V/rad	Phase-detector gain factor
$\omega_n = 141.43$ rad/s	Loop natural frequency
$T_p = 9.87E-02$ s	Pull-in time
$K_a = 62.89$	Required minimum amplifier gain
$\zeta = 0.707$	Damping factor
$T_1 = 3.14E-01$ s	Time constant of loop filter
$T_2 = 10.00E-03$ s	Time constant of loop filter
$C = 2.20$ $\mu$ F	Filter capacitor
$R_1 = 2.20$ k $\Omega$	Filter input resistor
$R_2 = 4.54$ k $\Omega$	Filter feedback resistor
$R_3 = 138.24$ k $\Omega$	Filter gain resistor
$R_0 = 138.24$ k $\Omega$	Amplifier offset resistor



Table 4. Static and Dynamic Power Performance of the Receiver

Case	Performance Parameter	MSK	GMSK
Static	$C/N_0^a$	44.3	44.8
With 100-Hz frequency offset, without AFC	$C/N_0$	48.8	----
With 100-Hz frequency offset, with AFC	$C/N_0$	44.3	44.8
Rician fading with LMR = 10, Doppler shift is 72 Hz, and LOS not shifted	$C/N_0$	47.3	47.8
Error floor, Rician fading with LMR = 10, Doppler shift is 72 Hz, and LOS not shifted	$P_e$	$10^{-6}$	----
Rician fading with LMR = 10, Doppler shift is 72 Hz, and LOS shifted 72 Hz	$C/N_0$	47.8	49.3
Error floor, Rician fading with LMR = 10, Doppler shift is 72 Hz, and LOS shifted 72 Hz	$P_e$	$0.7 \times 10^{-4}$	$10^{-4}$

<sup>a</sup>  $C/N_0$  is in dB.

also shifted by 72 Hz, the required  $C/N_0$  values for the MSK and GMSK signals are 47.8 and 49.3 dB, respectively. These figures are computed for an average error probability of 0.001.

## REFERENCES

- [1] F. Naderi, G. Knouse, and W. Weber, "NASA's Mobile Satellite Communications Program; Ground and Space Segment Technologies," Proc. 35th Annual International Astronautics Federation Congress, Lausanne, Switzerland, October 1984.
- [2] K. Murota and K. Hirade, "GMSK Modulation for Digital Mobile Radio Telephony," IEEE Trans. Commun., Vol. COM-29, pp. 1044-1050, July 1981.
- [3] K. Daikoku, K. Murota, and K. Momma, "High-Speed Digital Transmission Experiments in 920 MHz Urban and Suburban Mobile Channels," IEEE Trans. Veh. Technol., Vol. VT-31, pp. 70-75, May 1982.
- [4] S. Good, "A Comparison of Gaussian Minimum Shift Keying to Frequency Shift Keying for Land Mobile Radio," Proc. 34th Veh. Technol. Conf., Pittsburgh, Pennsylvania, pp. 136-141, May 1984.
- [5] H. Suzuki, K. Momma, and Y. Yamao, "GMSK Digital Portable Transceiver Using 32 kbps ADM," Proc. 33rd Veh. Technol. Conf., pp. 341-346, May 1983.
- [6] T. Masamura, S. Samejima, Y. Morihiro, and H. Fuketa, "Differential Detection of MSK with Nonredundant Error Correction," IEEE Trans. Commun., Vol. COM-27, pp. 912-918, June 1979.
- [7] K. Kinoshita, M. Hata, and H. Nagabuchi, "Evaluation of 16 kbit/s Digital Voice Transmission for Mobile Radio," IEEE Trans. Veh. Technol., Vol. VT-26, pp. 321-327, November 1984.
- [8] M. Simon and C. Wang, "Two Bit Differential Detection of MSK," Proc. GLOBCOM'84, Atlanta, Georgia, November 1984.
- [9] M. Simon and C. Wang, "Differential Detection of Gaussian MSK in a Mobile Radio Environment," IEEE Trans. Veh. Technol., Vol. VT-33, pp. 307-320, November 1984.
- [10] F. Davarian and J. Sumida, "Hardware Simulator Assists Mobile Satellite Experiment," Proc. 35th Veh. Technol. Conf., Boulder, Colorado, May 1985.
- [11] W. Vogel and E. Smith, Propagation Considerations in Land Mobile Satellite Transmission, JPL 9950-1050, Jet Propulsion Laboratory, Pasadena, California, January 1985.
- [12] F. Davarian, "Fade Margin Calculation for Channels Impaired by Rician Fading," IEEE Trans. Veh. Technol., Vol. VT-34, pp. 41-44, February 1985.